University of Bath

Alternative formats
If you require this document in an alternative format, please contact:
openaccess@bath.ac.uk

Transformation and sorption of illicit drug biomarkers in sewer biofilms

Pedram Ramin[a,b*], Andreas Libonati Brock[a], Ana Causanilles[c], Borja Valverde-Pérez[a], Erik Emke[c], Pim de Voogt[c,d], Fabio Polesel[a], Benedek Gy. Plósz[a,e,*]

[a]Department of Environmental Engineering, Technical University of Denmark (DTU), Bygningstorvet, Bygning 115, 2800 Kgs. Lyngby, Denmark

[b]Process and Systems Engineering Center (PROSYS), Department of Chemical and Biochemical Engineering, Technical University of Denmark, Building 229, 2800 Kgs. Lyngby, Denmark

[c]KWR Watercycle Research Institute, P.O. Box 1072, 3430 BB Nieuwegein, The Netherlands`1

[d]Institute for Biodiversity and Ecosystem Dynamics, University of Amsterdam, P.O. Box 94248, 1090 GE Amsterdam, The Netherlands

[e]Department of Chemical Engineering, University of Bath, Claverton Down, Bath BA2 7AY,UK

Corresponding authors: pear@kt.dtu.dk; b.g.plosz@bath.ac.uk

_____

Abstract

In-sewer transformation of drug biomarkers (excreted parent drugs and metabolites) can be influenced by the presence of biomass in suspended form as well as attached to sewer walls (biofilms). Biofilms are likely the most abundant and biologically active biomass fraction in sewers. In this study, 16 drug biomarkers were selected, including the major human metabolites of mephedrone, methadone, cocaine, heroin, codeine and tetrahydrocannabinol (THC). Transformation and sorption of these substances were assessed in targeted batch experiments using laboratory-scale biofilm reactors operated under aerobic and anaerobic conditions. A one-dimensional model was developed to simulate diffusive transport, abiotic and biotic transformation and partitioning

31   of drug biomarkers. Model calibration to experimental results allowed estimat-
32   ing transformation rate constants in sewer biofilms, which were compared to
33   those obtained using in-sewer suspended biomass.

34   Our results suggest that sewer biofilms can enhance the transformation of most
35   compounds. Through scenario simulations, we demonstrated that the estima-
36   tion of transformation rate constants in biofilm can be significantly biased if
37   the boundary layer thickness is not accurately estimated. This study comple-
38   ments our previous investigation on the transformation and sorption of drug
39   biomarkers in the presence of only suspended biomass in untreated sewage. A
40   better understanding of the role of sewer biofilms–also relative to the in-sewer
41   suspended solids–and improved prediction of associated fate processes can
42   lead to more accurate estimation of daily drug consumption in urban areas in
43   wastewater-based epidemiological assessments.

Introduction

45   Wastewater-based epidemiology (WBE) has emerged as a new paradigm to
46   monitor trends of community-wide drug use based on chemical analysis of uri-
47   nary drug biomarkers in raw sewage, typically in the influent of wastewater
48   treatment plants (WWTPs).[1,2] Transport in upstream sewer pipelines is known
49   to influence the quality of untreated wastewater[3], hence reliable estimations of
50   drug use based on observations in WWTP influents require consideration of
51   in-sewer transformations and sorption of biomarkers. A recent investigation[4]
52   in a full-scale pressurized sewer pipeline revealed significant elimination or
53   formation of pharmaceuticals (e.g. bezafibrate and sulfamethoxazole, respec-
54   tively).

55   The uncertainty introduced by neglecting in-sewer processes is often ignored[5]
56   among other sources of uncertainty in WBE studies.[6] The *in-sample* stability
57   of drug biomarkers has been widely assessed[7–10], providing an indication of
58   biotransformation in raw wastewater. These studies prominently addressed the
59   reliability of analysis after sample collection, focusing e.g. on biomarker sta-
60   bility during composite sample collections, rather than refining back-calcula-
61   tion schemes by accounting for in-sewer transformations. However, due to dif-
62   ferences in operation and design of sewer systems, *in-sewer* stability of drugs
63   of abuse is not only compound-specific but also highly dependent upon the
64   catchment layout (e.g., size[11]) and the hydraulic conditions in the pipelines.

65 Moreover, in-sewer fate processes are not limited to biotransformation in the
66 bulk phase and biofilms/sediments, but also include abiotic processes and par-
67 titioning of drug biomarkers to suspended and attached solids. Drug bi-
68 omarkers can be in-sewer transformation product of other human metabolites
69 and hence their concentration can be significantly influenced. When consider-
70 ing these challenges, chemical *stability* in terms of percentage removal effi-
71 ciency or correction factors (lumped factors that include excretion ratio, in-
72 sewer transformation etc.) cannot be a reliable source of information for the
73 estimation of drug load at the point of excretion.

74 Recently, transformation and sorption of several drug biomarkers in raw
75 wastewater in the presence of suspended biomass have been assessed using
76 targeted experiments and mechanistic modelling.[12] This previous study eluci-
77 dated the role of only one of the possible actors of in-sewer biochemical pro-
78 cesses, as biomass in sewer systems is present also in attached form. However,
79 limited evidence exists on the role of sewer biofilms. To date, only a few stud-
80 ies[13,14] assessed removal kinetics in sewer biofilms, showing enhanced relative
81 removal efficiency of selected drug biomarkers (cocaine and 6-mono-acetyl-
82 morphine) as compared to raw wastewater. Nevertheless, a number of previ-
83 ously uninvestigated factors are likely to influence (the estimation of) biofilm-
84 mediated transformation rates, namely (i) sorption onto biofilm[15], similarly to
85 suspended solids in untreated wastewater[12]; (ii) concurrent transformation and
86 formation from other biomarkers[8,12,16,17]; (iii) abiotic degradation[5,12]; (iv) pre-
87 vailing redox conditions (aerobic and anaerobic); and (v) diffusive transport
88 through boundary layer and in biofilm[15,18]. While being typically neglected in
89 biotransformation studies with biofilms, The impact of (v) may be substantial
90 considering the structure and the thickness of sewer biofilms and the reduced
91 diffusivity of large organic molecules.[19–21] This is especially important in pres-
92 surized sewers, where sewer biofilms are abundant in completely filled
93 pipes.[3,22]

94 In this study, we sought to improve the existing understanding of the fate of
95 drug biomarkers in the presence of sewer biofilms by means of an experimental
96 and model-based assessment. This study was meant to complement our previ-
97 ous investigation[12] on the fate of drug biomarkers in untreated sewage, in the
98 presence of only suspended biomass. The objectives of our investigation were
99 thus: (i) to assess the transformation and sorption of 16 drug biomarkers in
100 sewer biofilms under aerobic and anaerobic conditions (using laboratory-scale
101 rotating biofilm reactors); (ii) to model the fate of selected drug biomarkers in
102 the biofilm by explicitly describing diffusive transport and reaction kinetics;

3

103 (iii) to estimate biofilm-mediated biotransformation kinetics for the selected
104 biomarkers, and to compare them with transformation kinetics by suspended
105 biomass in untreated wastewater.

Materials and methods

107 **Selection of trace organic biomarkers.** Six illicit drugs were selected based
108 on their high consumption levels according to a recent European report.[23] The
109 target list was completed with 10 human metabolites and included: (i)
110 mephedrone (MEPH); (ii) methadone (METD) and its metabolite 2-ethylidene-
111 1,5-dimethyl-3,3-diphenylpyrrolidine (EDDP); (iii) cocaine (COC) and its me-
112 tabolites benzoylecgonine (BE), ecgonine methyl ester (EME), and co-
113 caethylene (CE); (iv) heroin (HER) and its metabolites 6-monoacetylmorphine
114 (6-MAM), morphine (MOR), and morphine-3-β-D-glucuronide (MORG); co-
115 deine (COE) and its metabolite norcodeine (NCOE); (v) tetrahydrocannabinol
116 (THC) and its metabolites 11-hydroxy-Δ9-THC (THCOH), and 11-nor-9-car-
117 boxy-Δ9-THC (THCCOOH). COE and NCOE were also considered in the
118 same group as MOR, since COE can potentially transform to MOR and NCOE
119 during human metabolism.[24] Analytical Standards (IS) and isotopically labeled
120 internal standard (ILIS) analogues from Sigma Aldrich (Brøndby, Denmark)
121 were dissolved in methanol or acetonitrile at concentrations of 0.1 mg mL^{-1}
122 and 1 mg mL^{-1}, respectively. Poor data quality prevented us from assessing the
123 transformation of methamphetamine and amphetamine, which are widely used
124 in Europe.[23]

125 **Experimental set-up with continuous-flow operation.** Two annular rotating
126 biofilm reactors, made of poly(methyl methacrylate) (Plexiglas), operated ei-
127 ther under aerobic or anaerobic conditions with operating volume of 0.961 L,
128 were used to simulate in-sewer conditions by controlling, e.g., shear conditions
129 on biofilm. The reactors consisted of an inner rotating drum (diameter=9.0 cm)
130 and an outer stationary cylinder (diameter=11.4 cm), supporting the growth of
131 attached biomass. This type of reactor provided for high surface area to volume
132 ratio (175 m^2 m^{-3}) that could be advantageous for biofilm growth. Each reactor
133 was equipped with four removable slides, allowing for inspection of biofilm
134 during reactor operation.

135 In order to establish stable aerobic and anaerobic biofilms, the two reactors were
136 operated under continuous-flow conditions for more than 7 months while being
137 kept in the dark. The rotation speed of the reactors was set to 20 rpm. The wall
138 shear stress was calculated according to equations provided by Rochex et al.[25] as

139   0.05 Pa which is in the lower range of typical wall shear stress in the sewers, meas-
140   ured up to 3 Pa in a gravity sewer.[26] Low shear stress was chosen in order to de-
141   crease biofilm sloughing and therefore enhance biofilm thickness. The reactors
142   were continuously fed (4 L d^{-1}, hydraulic residence time of approximately 0.25
143   d^{-1}) with pre-clarified wastewater from external cooled containers (T ≤ 4°C)
144   that were sparged with dry compressed atmospheric air (aerobic reactor) or
145   nitrogen (anaerobic reactor). The experiments were performed to mimic com-
146   pletely aerobic and anaerobic redox conditions. The external tanks were filled with
147   pre-clarified wastewater collected from Mølleåværket WWTP (Lundtofte, Den-
148   mark) semi-weekly. The wastewater had following characteristics: soluble organic
149   carbon, expressed as chemical oxygen demand (COD) = 40–130 g m^{-3}, total COD
150   (120–g m^{-3}), biological oxygen demand (BOD) = 90–200 g m^{-3}, nitrate < 1 gN m^{-}
151   ^{3}, total nitrogen (TN) = 20–50 gN m^{-3}, sulfate = 12-55 gS m^{-3}.
152
153   **Laboratory-scale batch experiments.** Following long-term continuous-flow
154   operation, two sets of batch experiments were performed: (i) biotransformation
155   experiments with intact biofilm in rotating reactors (BT); and (ii) sorption ex-
156   periments with re-suspended biofilm (SO). All experiments were started (t=0)
157   three minutes after spiking of biomarker standard solutions to ensure mixing
158   of spiked biomarkers in solution. Figure 1 illustrates the reactor configuration
159   and operation during BT Experiments. During the entire operation, the biofilm
160   reactors were kept full and intermittent wetting was avoided to prevent reduc-
161   tion of the overall activity of the biofilm. A detailed description of each set of
162   batch experiments is provided below. Description of all batch experiments is
163   also presented in SI Table S2.

164   *Biotransformation experiments (BT).* Each rotating biofilm reactor was con-
165   nected to an external container with a recirculating flow of 4 L h^{-1}. This con-
166   figuration allowed for sample collection from the external container without
167   changing the operating volume of the biofilm reactors. Two procedures were
168   considered. The first procedure (BT-P1) was conducted by spiking a mixture
169   containing all IS to obtain an initial (t=0) concentration of 10 µg L^{-1}. Following
170   sample withdrawal during experiments, samples were immediately spiked with
171   a mixture containing ILIS. The IS solution mixture contained the main target
172   compounds and ILIS were used to evaluate the analytical procedure. The sec-
173   ond procedure (BT-P2) was conducted by spiking ILIS at initial (t=0) concen-
174   tration of 2 µg L^{-1}. In this second case only ILIS were spiked and considered
175   the target compounds, including only MEPH-d3, METD-d3, EDDP-d3, COC-
176   d3, BE-d3, EME-d3, CE-d3, HER-d9 and 6MAM-d3. This procedure allowed

177 for the improved determination of illicit drug analytes without interference of
178 background concentrations (SI, Figure S3).[13]

179 The duration of the experiments was two days, during which 9 samples for BT-
180 P1 and 12 samples for BT-P2 experiments were collected (around 260 mL sam-
181 ple volume, see SI, Figure S2). During BT-P1 experiments, additional samples
182 were collected (i) before biomarker spiking, to measure the background con-
183 centrations; and (ii) during experiments, to monitor the biological activity of
184 the biofilms via measurements of chemical oxygen demand (COD), sulfate
185 (SO_4-S), ammonium (NH_4-N) and nitrate (NO_3-N).

186 BT-P1 and BT-P2 experiments were conducted after continuous-flow opera-
187 tion of biofilm reactors for 14 and 7 months, respectively assuming biofilm
188 reached maximum thickness. In this study, results of BT-P1 and BT-P2 exper-
189 iments were used for model identification/calibration (i.e., estimation of ki-
190 netic parameters and identification of transformation pathways) and for model
191 evaluation, respectively. For BT-P1 experiments (aerobic: pH=8.7±0.1,
192 T=17±0.3 °C; anaerobic: pH=9.2±0.4, T=17.8±0.5 °C), and BT-P2 experi-
193 ments (aerobic: pH=8.8±0.06, T=17.6±0.2 °C; anaerobic: pH=8.7±0.2,
194 T=17.5±0.4°C), wastewater was collected from Mølleåværket WWTP
195 (Lundtofte, Denmark). Collected pre-clarified wastewater was centrifuged (20
196 min, 4700 rpm) and vacuum filtered (Advantec MFS, Inc., GA-55 grade) for
197 removal of suspended solids.

198 *Sorption experiments (SO).* Sorption experiments (SO) were performed with
199 suspended aerobic biofilms (SO1) and suspended anaerobic biofilms (SO2).
200 The experiments were conducted after 14 months of continuous-flow operation
201 of the biofilm reactors. Tap water was circulated through the biofilm reactors
202 for 17 h to wash-off already sorbed compounds in the biofilm. Two slides were
203 removed from each reactor and intact biofilm was suspended in 2 L tap water
204 for 4 h for further desorption. After centrifugation (30 min, 4700 rpm), the
205 separated solids were mixed with 4 L vacuum filtered (Advantec MFS, Inc.,
206 GA-55 grade, pore size 6 μm) wastewater effluent (Mølleåværket WWTP,
207 Lundtofte, Denmark). To inactivate biomass during experiment, sodium azide
208 (0.05% v/v) was added to the mixture. The experiments were conducted for 4
209 h after spiking standard mixture and in total six samples (260 mL) were with-
210 drawn. During SO1 experiment (pH=7.9±0.1, T=15.4±0.2°C) and SO2 exper-
211 iment (pH=7.9±0.1, T=15.3±0.1 °C), the reactors were sparged with dried com-
212 pressed air and nitrogen, respectively.

Biofilm characterization. The biofilm thickness (aerobic: 0.75 mm; anaerobic: 1.02 mm) was calculated by measuring biofilm volume and considering the reactor surface area of 1679 cm^2. The biofilm volume was measured by filling the rotating reactors with tap water without and with biofilm inside the reactors. The difference between the volume of the empty reactor without biofilm (961 cm^3) and the free volume of the reactors with biofilm (aerobic reactor, 836 cm^3; anaerobic reactor, 790 cm^3) was considered as the wet biofilm volume. The solids content of the biofilm was measured by re-suspending the biofilm on two removable slides into tap water, and subsequently measuring total suspended solids (TSS) and volatile suspended solid (VSS) of the mixture. The total dried mass per biofilm volume in the reactors, defined as biofilm density, was then calculated (aerobic reactor, 55 gTSS L^{-1}, 22 gVSS^{-1} L^{-1}; anaerobic reactor, 83 gTSS L^{-1}, 38 gVSS^{-1} L^{-1}).

Sample preparation and chemical analyses. Total suspended solids (TSS) were measured using gravimetric analysis after filtration (0.6 μm glass fiber filter, Advantec, USA).[27] Total and soluble COD, nitrate, ammonium and sulfate were measured using colorimetric methods (Hach Lange and Merck, Germany). For dissolved components, the analyses were carried out after sample filtration (0.45 μm cellulose acetate filters, Sartorius, Germany) and storage at -20 °C.

For the analysis of drug biomarkers (one sample at each sampling time), a description of sample preparation and chemical analysis by liquid chromatography coupled to high resolution mass spectrometry (HPLC-LTQ-Orbitrap) can be found elsewhere.[12,28] Briefly, samples were collected and immediately frozen until analysis. For samples from SO experiments samples were first filtered (0.6 μm glass fiber filter, Advantec, USA) to reduce the contact time between solids and liquid phase. Later, samples were thawed and homogenized, and 100 mL aliquots were extracted by solid phase extraction with Oasis HLB cartridges (150 mg, 6 cc, Waters, Denmark). Extracts were reconstituted in water:methanol (90:10, v/v) and 20 μL were injected into the HPLC-LTQ-Orbitrap. Separation of the target compounds was achieved in an XBridge C18 column (150 mm × 2.1 mm, I.D., particle size 3.5 μm; Waters) with a MiliQ and MeOH optimized gradient (each with 0.05% formic acid). Full scan accurate mass data were acquired in positive electrospray ionization mode over a m/z range of 50–600 Da at a resolution of 30000 full width at half maximum. For confirmation purposes, information about the fragmentation spectra of the target compounds was obtained by product-ion scan mode of the target masses

250 inclusion list, in the same analysis. All data were acquired and processed using
251 Xcalibur version 2.1 software.

252 **Modeling framework.** The mathematical description of fate processes was
253 formulated by accounting for temporal and spatial variation of target analyte
254 concentrations in biofilms. Due to mass transfer limitation from the bulk phase
255 to the biofilm and within the biofilm, concentration gradients can occur in the
256 biofilm reactors. For the specific case of batch experiments, it was assumed
257 that the biofilm is at steady state and as a homogeneous biomass. The volume
258 inside the biofilm reactors was constant, whereas in the external tank the vol-
259 ume decreased due to withdrawal of samples. Thus, the contact time between
260 the dissolved compounds in liquid phase and biofilm increased, which could
261 potentially enhance biomarker transformation. Consequently, residence time
262 dynamics were also included in the model by accounting for volume changes
263 in the external tank (SI Figure S2). As illustrated in Figure 1, the experimental
264 system consists of three compartments: (i) the bulk liquid in the rotating reac-
265 tor, (ii) the biofilm in the rotating reactor and (iii) the external tank (continu-
266 ously stirred tank reactor) connected to the biofilm reactor via a peristaltic
267 pump. The differential equations describing mass balances in each compart-
268 ment can be formulated as follows (all model parameters and state variables
269 are listed in Table 1):

270 i) In the biofilm reactor bulk phase:

271 $$\frac{d\,V_R C_{R,i}}{dt} = Q_{in,R} C_{in,R,i} - Q_{out,R} C_{R,i} - j_b A_b + r_{R,i} V_R \qquad \text{(eq.1)}$$

272 ii) In the biofilm:

273 $$\frac{\partial\,V_b C_{b,i}}{\partial t} = A_b D \frac{\partial^2 C_{b,i}}{\partial z^2} \Delta z + r_{b,i} V_b \qquad \text{(eq. 2)}$$

274 iii) In the external tank:

275 $$\frac{d\,V_T C_{T,i}}{dt} = Q_{in,T} C_{in,T,i} - Q_{out,T} C_{T,i} + r_{T,i} V_T \qquad \text{(eq. 3)}$$

276 In these formulations, C (g m^{-3}) denotes the concentration as state variable and
277 the subscripts R, b and T indicate bulk phase of the rotating reactor, the biofilm,
278 and the external tank, respectively. The volume, which is constant for the re-
279 actor bulk phase V_R (m^{-3}) and the biofilm V_b (m^{-3}), changes as a function of
280 time inside the external tank, V_T (m^{-3}), as previously explained.

8

281   *Transport processes.* The flux of compounds between bulk phase and the bio-
282   film, j_b (g m^{-2} d^{-1}), is expressed using film theory at the mass transfer boundary
283   layer[29]. The flux of compounds across the boundary layer can be defined as:

284     $$j_b = k_b(C_R - C_L) = \frac{D}{L_b}(C_R - C_L) \qquad\qquad \text{(eq. 4)}$$

285   Where k_b (m d^{-1}) is the liquid-biofilm mass transfer coefficient, D (m^2 d^{-1}) is
286   the diffusion coefficient of the dissolved compounds into the biofilm, L_b (m) is
287   the biofilm thickness, and C_L is the concentration at the biofilm-liquid interface
288   (top layer). It was assumed that no reactions occur in the boundary layer. The
289   diffusion coefficients of target biomarkers in water, D_w (m^2 d^{-1}) were calculated
290   based on the revised Othmer-Thakar[30] equation suggested by Hayduk and
291   Laudie[31]:

292     $$D_w = \frac{13.26\,(10^{-5})}{\mu_w^{1.4} V_1^{0.589}}\,, \qquad\qquad \text{(eq. 5)}$$

293   where μ_w (kg m^{-1} s^{-1}) denotes the dynamic viscosity of water and V_1 (cm^3 g
294   mole^{-1}) is the molar volume of the substance. Diffusion coefficients (D_W) cal-
295   culated using eq. 5 are reported in Table S1. Diffusion coefficients inside the
296   biofilm were assumed to be reduced as compared to bulk water phase. Reduced
297   effective diffusivity results from limitation due to increased path length in bio-
298   film pores as compared to free aqueous media. Consequently, a dimensionless
299   effective diffusivity factor, f, was considered:

300     $$D = f D_w \qquad\qquad \text{(eq. 6)}$$

301   The value of f was approximated by considering the density of the biofilm as
302   VSS (gVSS L^{-1}), based on the regression presented by Guimerà et al.[32] The
303   boundary layer thickness, L_b, was estimated using dimensionless numbers, [33,34]
304   namely Sherwood number (*Sh*), Schmidt number (*Sc*), Taylor number (*Ta*) and
305   Reynolds number (*Re*), (see SI, eqs. S1 to S4).

306   *Reaction processes.* Reaction kinetics in the bulk phase of the biofilm reactor
307   includes abiotic processes and biotransformation due to the presence of sus-
308   pended biomass. The amount of suspended solids was the residuals of solids
309   that remained in filtered wastewater (measured at t=0) and amount of detached
310   biomass assumed to be negligible. These processes were formulated according
311   to the Activated Sludge Model for Xenobiotics (ASM-X) framework.[12,16] The
312   reaction rate for transformation of compound i and its formation from com-
313   pound j can be formulated as:

314 $$r_{R,i} = -k_{abio}C_{R,i} + k_{abio}C_{R,j}\frac{M_i}{M_j} - \frac{k_{bio}X_{SS}}{(1+K_{d,i}X_{SS})}C_{R,i} + \frac{k_{bio}X_{SS}}{(1+K_{d,j}X_{SS})}C_{R,j}\frac{M_i}{M_j}$$

315 (eq. 7)

316 Where k_{abio} (d^{-1}) is the abiotic transformation rate, k_{bio} (L gTSS^{-1} d^{-1}) is the
317 TSS-normalized biotransformation rate constant for the suspended solids, K_d
318 (L gTSS^{-1}) is the partitioning coefficient to suspended solids X_{SS} (g L^{-1}), and M
319 is the molecular weight. Equilibrium processes were assumed for sorption and
320 desorption onto suspended solids.

321 Inside the biofilm, in addition to abiotic processes, transformation and for-
322 mation processes resulted from the microbial activity of the attached biomass.
323 The associated kinetic equations were expressed as:

324 $$r_{b,i} = -k_{abio}C_{R,i} + k_{abio}C_{R,j}\frac{M_i}{M_j} - k_{f,i}C_{b,i} + k_{f,j}C_{b,j}\frac{M_i}{M_j}$$ (eq. 8)

325 $$k_{f,j} = \frac{k_{biof,j}X_{SS}}{(1+K_{df,j}X_{SS})}$$ (eq. 9)

326 In this formulation, biofilm-mediated transformation (subscript f) is expressed
327 using pseudo-first order kinetics, where k_f and k_{biof} are in units of d^{-1} and L
328 gTSS^{-1} d^{-1}, respectively, and K_{df} (L gTSS^{-1} d^{-1}) is the partitioning coefficient in
329 biofilms. Biofilm-mediated transformation can also be expressed by surface-
330 normalized rate constants k'_{biof} (m^3 m^{-2} d^{-1}), obtained by dividing k_{biof} with
331 $X_{SS}\cdot\times A_b/V_b$. The units of the reactions rates were adjusted to g m^3 d^{-1} according
332 to the units in eq. 1-3.

333 Finally, the reaction kinetics in the external tanks were assumed to be the same
334 as in the bulk aqueous phase of the biofilm reactor, with additional processes
335 for sorption and desorption to and from the tank wall[12]:

336 $$r_{T,i} = r_{R,i} - k_{des,w}k_{d,w}C_{T,i}\frac{A_T}{V_T} + k_{des,w}C_{Tw}$$ (eq. 10)

337 Where C_{Tw} (g L^{-1}) denotes the biomarker concentration sorbed onto reactor
338 wall, $K_{d,w}$ (m^3 m^{-2} d^{-1}) the partitioning coefficient to reactor wall. and $k_{des,w}$ (d^{-1}
339 ^{1}) is the desorption rate from the reactor wall.

340 **In-sewer transformation pathways.** Transformation and formation processes
341 defined in eqs. 7–10 depend on the pathways identified for abiotic processes,
342 transformation due to presence of suspended solids and biofilm-mediated
343 transformations. The first two were adopted from our previous study.[12] Trans-
344 formation pathways in biofilms were initially assumed based on reported hu-
345 man metabolic pathways.[7,35] This initial assumption was required due to the

346   absence of a priori evidence and was tested as part of the modelling study.
347   Subsequently, any deviation from the initial pathways was assessed by exam-
348   ining the mass balance over suggested transformed compounds and observed
349   transformation products (according to human metabolism).

350   **Model parameter estimation.** The values employed for k_{abio} and k_{bio} for sus-
351   pended biomass in bulk phase were estimated in an another study.[12] Using SO1
352   and SO2 measurements (SI, Figure S8) the K_{df} values were estimated accord-
353   ing to Ramin et al.[12] Values of k_f were estimated using the Bayesian optimiza-
354   tion method Differential Evolution Adaptive Metropolis (DREAM$_{(ZS)}$).[36] The
355   normalized sum of squared error (SSE) was used as objective function:

356
$$SSE = \sum_{i=1}^{n} \sum_{j=1}^{m} \left(\frac{O_{i,j} - P_{i,j}}{O_{i,j,\max} - O_{i,j,\min}} \right)^2 \qquad \text{(eq. 11)}$$

357   Where n is the number of measurements series and m is the number of the data
358   points in each series. O denotes measured data, P model predictions, and $O_{i,j,max}$
359   and $O_{i,j,min}$ the maximum and minimum of measurements, respectively. To ad-
360   equately quantify the uncertainty associated to the k_f estimates, the uncertainty
361   from k_{abio} and k_{bio} was propagated according to the identified transformation
362   pathways for abiotic processes and biotransformation in presence of suspended
363   solids.[37] Values of k_{biof} were eventually estimated based on eq. 9. We consid-
364   ered an upper boundary threshold of 10^4 d^{-1} for k_f in parameter estimation. Pa-
365   rameter estimates beyond this threshold were considered to result from model
366   structure deficiencies (related to mass transfer).

367   **Model simulation and evaluation.** To simulate the transformation processes,
368   eqs. 1–3 were numerically solved following a spatial discretization of the bio-
369   film. Theoretically, increasing the discretization level (grid points) would in-
370   crease the accuracy of prediction at the expense of higher computational time.
371   For central grids (inside the biofilm), discretization was done using the central
372   difference formula. Values at the first grid (biofilm-liquid interface) and the
373   last grid points were computed via forward and backward difference, respec-
374   tively. This discretization scheme was adopted from the biofilm simulation
375   model developed by Vangsgaard et al.[38] The resulting set of ordinary differen-
376   tial equations was solved using the stiff ODE solver ode15s in Matlab R2014a
377   (MathWorks, US). Model parameter uncertainty was assessed using the poste-
378   rior probability distribution of estimates in Monte Carlo simulations as ex-
379   plained elsewhere.[39] Subsequently, the accuracy of the predictions was visually

11

380 evaluated comparing measurements from BT-P2 experiments, i.e. an independ-
381 ent dataset, with model predictions.

Results and discussion

Biological activity of biofilm reactors. To monitor microbial activity in aer-
obic and anaerobic biofilms, soluble COD, sulfate and ammonium (Figure 2)
as well as total COD and nitrate (SI, Figure S4) were monitored in the bulk
phase during the BT-P1 experiments (while reactors were disconnected from
continuous feeding). Soluble COD consisted of readily biodegradable organic
substrates and soluble inert fractions, including MeOH present in the spiking
solution. Utilization of MeOH as growth substrate was assumed to be negligi-
ble as in our previous study[12] we did not observe any substantial difference in
suspended biomass growth and oxygen uptake response upon MeOH addition.
Due to the likely higher activity of heterotrophic biomass under aerobic con-
ditions as well as higher MeOH evaporation rate (dried air was sparged at a
higher flow rate in the external tank compared to nitrogen gas), higher removal
of soluble COD was observed in the aerobic reactor (88%) compared to the
anaerobic one (57%) over 2 d. Due to the activity of sulfate reducing bacteria
(SRB), sulfate was significantly reduced under anaerobic conditions (62% over
1 d) and remained constant during last day of experiment (Figure 2b). This may
indicate that sulfate respiration by SRB species was limited by the absence of
readily biodegradable substrate during the second day of experiment. Under
aerobic conditions, the net formation (+33%) of sulfate was observed over 2 d,
possibly due to biochemical oxidation of hydrogen sulfide (H_2S) back to sul-
fate. In the aerobic BT-P1 reactor, ammonium removal is possibly dominated
by assimilatory ammonia uptake. It is also reported that nitrifiers are usually
overgrown by heterotrophic biomass in sewer biofilms (Huisman and Gujer,
2002; Jiang et al., 2009). Under anaerobic conditions, ammonium removal
could be due to assimilation and stripping – latter due to the comparably high
pH (9.2).

409

Partitioning of drug biomarkers to biofilm. Two solid-liquid partitioning coefficients were estimated for aerobic ($K_{df,ae}$) and anaerobic biofilms ($K_{df,an}$) using SO1 and SO2 experimental data, respectively (SI Figure S8). In addition, abiotic chemical transformation was assessed in mineral water spiked with the selected biomarkers – a study carried out previously.[12] These data were considered to disregard the contribution of abiotic transformation during sorption experiments. Estimated partitioning coefficients are reported in SI Table S4. The highest sorption capacity was found for THCOH ($K_{df,ae}$=2.81 L gTSS^{-1}; $K_{df,an}$=1.68 L gTSS^{-1}). The drop in THC concentration in the sorption experiments (72% in aerobic biofilms and 58% in anaerobic biofilm) can be interpreted as a result of chemical partitioning to external tank wall, as it was observed previously[12], with the K_{df} values being negligible despite the high hydrophobicity of this chemical ($logK_{ow}$=7.6).[40] However, given the high hydrophobicity of THC, high sorption onto biofilm solids could not be ruled out, and further experimental confirmation may be required to verify our findings. Sorption of THCCOOH, EME and EDDP was only observed for anaerobic biofilms ($K_{df,an}$=1.06 L gTSS^{-1}; 1.59 L gTSS^{-1}; $K_{df,an}$=0.15 L gTSS^{-1} respectively). Conversely, partitioning under aerobic conditions was found for MEPH ($K_{df,ae}$=0.20 L gTSS^{-1}). For the remaining chemicals, negligible sorption was observed, hence K_{df} values were set to zero. Notably, the anaerobic biofilm had higher thickness and density compared to the aerobic biofilm, which may explain the selective sorption of some of the drug biomarkers.

Transformation of drug biomarkers. Measurements from BT-P1 experiments were used to calibrate developed 1-D model and to predict temporal and spatial concentration profiles of drug biomarkers in the presence of sewer biofilms. Biotransformation due to the presence of suspended solids was accounted for by including previously estimated k_{bio} (L gTSS^{-1} d^{-1})[12,37] (SI, Table S3). Measured TSS concentrations in the bulk were considered constant, namely, 42 mgTSS L^{-1} and 104 mgTSS L^{-1} (for BT-P1 aerobic and anaerobic, respectively) 92 mgTSS L^{-1} and 80 mgTSS L^{-1} (for BT-P2 aerobic and anaerobic, respectively). The abiotic transformation rates k_{abio} and partitioning coefficients of drug biomarkers to suspended solids, K_d (L gTSS^{-1}), were set at values reported in SI, Table S3.[12] Subsequently, biofilm-mediated biotransformation rates k_f (d^{-1}) and rate constants k_{biof} (L gTSS^{-1} d^{-1}) and k'_{biof} (m^3 m^{-2} d^{-1}) were estimated.

Measured and simulated concentration profiles of all targeted biomarkers, obtained through model calibration and validation, are presented in Figure 3. Experimental and simulation results describe removal and formation of selected

448 drug biomarkers in the bulk phase of the biofilm reactor, where samples were
449 collected. The simulation results obtained through model calibration are pre-
450 sented using the median of the estimated parameters (full and dash lines) with
451 the corresponding 95% credibility interval (shaded uncertainty band). The un-
452 certainty boundary ranges, shown in Figure 3, were obtained through the prop-
453 agation of the uncertainties from abiotic and biotic transformation rates (quan-
454 tified here or previously[12]) to the model outputs. The transformation pathways
455 identified in this study are presented in Figure S6–7. Parameter values esti-
456 mated (reported as median ± credibility interval) are listed in Table S5 and all
457 posterior distributions of k_f values are given in Figure S11. Experimental and
458 modelling results are presented and discussed in detail for each group of chem-
459 icals in the following paragraphs.

460 Prior to estimating values of k_f, the impact of discretization number (i.e. the
461 number of layers in which the biofilm is discretized) on the prediction accuracy
462 was assessed. The case of the aerobic transformation rates for MEPH, $k_{f,ae,MEPH}$,
463 and HER, $k_{f,ae,HER}$, is discussed in detail (Figure 4, X-Z axis; Figure S5). HER
464 and MEPH were chosen because they represent compounds with low and high
465 removal rate, respectively. Discretization numbers, selected in the interval of
466 5-100 layers, were used to estimate k_f and using the highest level used to bench-
467 mark the level of error introduced by inaccurate model simulations. The dif-
468 ference is reported as relative percentage error, in which best-fit estimates for
469 $k_{f,ae,HER}$ and $k_{f,ae,MEPH}$ were compared with their corresponding reference values,
470 214.1 d^{-1} and 24.3 d^{-1}, respectively. It was observed that the number of dis-
471 cretization had a different impact on the estimated k_f of these two chemicals,
472 and that after 80 grid points the resulting error was negligible (< 1 %) and
473 independent of the discretization number. This discretization number corre-
474 sponds to ΔZ=9.3 μm and ΔZ=12.8 μm for aerobic and anaerobic biofilms,
475 respectively.

476 *Mephedrone.* MEPH removal was more pronounced in the aerobic reactor
477 (77% versus 47% in the anaerobic reactor). Higher partitioning to aerobic bio-
478 films resulted in much higher biotransformation rate constants under aerobic
479 conditions ($k_{biof,ae,MEPH}$=5.89 L gTSS^{-1} d^{-1}, $k_{biof,an,MEPH}$=0.08 L gTSS^{-1} d^{-1}). The
480 comparably high sorption of MEPH in aerobic biofilms ($K_{df,ae}$=0.2 L gTSS^{-1})
481 makes this compound less bioavailable for microbial transformation. This im-
482 pact is also reflected in eq. 9, in which k_{biof} is in the numerator and K_{df} is in
483 denominator. Moreover, the higher aerobic k_{biof} obtained in this study agrees
484 well with those reported previously[12] ($k_{bio,ae,MEPH}$=1.86 L gTSS^{-1} d^{-1},

14

485 $k_{bio,an,MEPH}$=0 L gTSS^{-1} d^{-1}). The model could adequately simulate BT-P2 da-
486 taset under both redox conditions, thereby validating the process model struc-
487 ture identified.

488 *Methadone.* Since formation of EDDP after rapid removal of METD, especially
489 under aerobic conditions, was not observed (Fig. 3), these chemicals were consid-
490 ered to have independent pathways – similar to that obtained with suspended in-
491 sewer solids.[12] Our analyses showed rather small deviation between duplicates
492 (sample analysis), i.e. ≤7.5% for METD and ≤4.5% for EDDP.
493 Biotransformation of METD in sewer biofilms was found to be significantly
494 faster under aerobic conditions ($k_{biof,ae,METD}$=2488 L gTSS^{-1} d^{-1}, $k_{biof,an,METD}$=183
495 L gTSS^{-1} d^{-1}), which agrees well with data obtained with in-sewer suspended
496 solids.[12] Conversely, enhanced anaerobic transformation was observed for
497 EDDP ($k_{biof,ae,EDDP}$=1.79 L gTSS^{-1} d^{-1}, $k_{biof,an,EDDP}$=88.9 L gTSS^{-1} d^{-1}). Simula-
498 tion results (Fig. 3) for EDDP (both redox conditions) as well as for METD
499 (only anaerobic conditions) indicate a systematic deviation between the pre-
500 dicted and measured values. This may imply that the model structure should
501 be re-evaluated in future studies. A possible explanation could be related to
502 cometabolic effects, i.e. primary substrate oxidation can enhance secondary
503 substrate (i.e. drug biomarker) biotransformation.[41–43] Additionally, under an-
504 aerobic conditions, the sulfate remained constant after day 1 (Figure 2b). This
505 may suggest that readily biodegradable substrates were depleted during the
506 second day of experiment, resulting in negligible removal of EDDP and
507 METD. Nevertheless, simulations could not well predict the BT-P2 dataset es-
508 pecially for METD, in which lower removal was observed as compared to BT-
509 P1 measurements, as the process model do not account for cometabolic effects.

510 *Cocaine.* The transformation pathways for COC and its human metabolites
511 were selected based on Bisceglia et al.[44] Although the biotransformation of
512 COC to EME has been reported to be almost insignificant in raw wastewater
513 and activated sludge[16,45], in this study EME was considered as a transformation
514 product (Fig. S6d) of COC in sewer biofilms. Accordingly, it has been reported
515 that, in sewer biofilms, there should be another major transformation product
516 from COC other than BE as it was speculated previously.[13] Net removal of
517 COC, CE and EME and net formation of BE was observed over the duration of
518 experiments, where BE formation resulted from hydrolysis of COC and CE.[12,44]
519 Under aerobic conditions, the overall biotransformation rate constant of COC,
520 i.e. COC to BE and COC to EME, was lower than under anaerobic conditions
521 ($k_{biof,ae,COC}$=0.44 L gTSS^{-1} d^{-1}, $k_{biof,an,COC}$=2.57 L gTSS^{-1} d^{-1}). An even more
522 pronounced deviation was observed for EME ($k_{biof,ae,EME}$=0.05 L gTSS^{-1} d^{-1},

$k_{biof,an,EME}$=21.03 L gTSS^{-1} d^{-1}), mainly due to the high biotransformation of EME in the bulk phase under aerobic conditions, SI Table S3. Aerobic and anaerobic percentage removal of COC only by sewer biofilms was found to be 3% and 33% larger than the removal observed in raw wastewater under corresponding redox conditions.[12] In contrast, Thai et al.[13] found 25% and 40% enhancement of COC removal in gravity sewer (aerobic/anaerobic) and rising sewer (anaerobic) conditions, respectively compared to removal with wastewater only. In our study, CE biotransformation kinetics obtained under aerobic and anaerobic biofilms were comparable ($k_{biof,ae,CE}$=0.68 L gTSS^{-1} d^{-1}, $k_{biof,an,CE}$=0.51 L gTSS^{-1} d^{-1}). BE is formed from COC and CE transformations and also transformed to another unknown transformation product ($k_{biof,ae,BE}$=2.00 L gTSS^{-1} d^{-1}, $k_{biof,an,BE}$=0.95 L gTSS^{-1} d^{-1}). Values of k'_{biof} (m^3 m^{-2} d^{-1}) estimated in this study (SI, Table S4) for overall COC, BE and CE for aerobic biofilms ($k'_{biof,ae,COC}$=0.13 m^3 m^{-2} d^{-1}, $k'_{biof,ae,BE}$=0.57 m^3 m^{-2} d^{-1}, $k'_{biof,ae,CE}$=0.39 m^3 m^{-2} d^{-1}) are almost 4 times, 34 and 2 times higher than the values reported by McCall et al.[14] (aerobic biofilms at 21°C). In contrary, for BE, no transformation by in-sewer suspended solids and sewer biofilms was reported.[13] The differences are possibly due to different microbes residing in the biofilms in these studies.

Heroin. Transformation of heroin biomarkers was assumed to follow the pathways previously described for human metabolism[24,35,46], namely two-step deacetylation to 6MAM and to MOR. MORG was also considered to be transformed to MOR via deconjugation.[47] It was hypothesized that COE was not only transformed to NCOE by sewer biofilms but also to MOR as it was observed in raw wastewater under anaerobic conditions.[37] Nevertheless, biofilm-mediated biotransformation processes could be described with transformation pathways similar to human metabolism. HER was rapidly removed in both sewer biofilms (similarly to raw wastewater (SI, Figure S9), with higher biotransformation kinetics in anaerobic biofilms ($k_{biof,ae,HER}$=4.43 L gTSS^{-1} d^{-1}, $k_{biof,an,HER}$=22.14 L gTSS^{-1} d^{-1}). Likewise, a five-fold increase of 6MAM biotransformation kinetics was observed in anaerobic biofilms ($k_{biof,ae,6MAM}$=1.11 L gTSS^{-1} d^{-1}, $k_{biof,an,6MAM}$=6.45 L gTSS^{-1} d^{-1}). These differences cannot be explained only by considering differences in the removal of 6MAM in aerobic and anaerobic biofilms (i.e. 33% and 59% in aerobic and anaerobic biofilms in 12 h experimental time (SI, Figure S9). Thus, additional processes are assumed to be involved, notably, the formation of 6MAM from HER. Given that the 6MAM biotransformation by in-sewer suspended solids is significantly lower than in biofilms, the total % removal is not substantially different from those

16

561 reported by Thai et al.[13] However, McCall et al.[14] found 3 times higher bio-
562 transformation rate for 6MAM by aerobic biofilm compared to in-sewer sus-
563 pended solids. In this study, as to pathway identification, no additional trans-
564 formation product of HER was considered when assessing the conservation of
565 HER mass. Moreover, MORG was found to be transformed only by anaerobic
566 sewer biofilm ($k_{biof,an,MORG}$ =2.03 L gTSS^{-1} d^{-1}) – a rate approximately 6 times
567 lower than that by in-sewer suspended biomass.[12] Due to rapid aerobic trans-
568 formation of MORG in the bulk, no aerobic biofilm-induced removal was ob-
569 served for MORG. High transformation of MORG was also observed by Senta
570 et al.[8] in wastewater.

571 Biotransformation rates obtained for COE and NOE in biofilms are at a mod-
572 erate level, with NCOE having higher transformation under anaerobic condi-
573 tions. The simulation model identified can effectively simulate the fate of HER
574 and 6-MAM transformation in the BT-P2 independent datasets, thereby vali-
575 dating the modelling approach.

576 *THC.* In untreated wastewater, THCOH was not found to be a transformation
577 product of THC.[12] Accordingly separate transformation pathways were as-
578 sumed for THC and THCOH in sewer biofilms. Based on pathways suggested
579 in literature,[35] THCCOOH was considered to be formed from THCOH.[35] As a
580 result of poor data quality, no clear conclusion could be drawn for THC bio-
581 transformation especially under anaerobic conditions. Moreover, the
582 $k_{biof,ae,THC}$=0 as THC removal was completely attributed to partitioning to the
583 external tank and abiotic hydrolysis. Hence, model calibration could not be
584 performed using THC data set (SI, Figure S10). THCOH exhibited comparably
585 high biotransformation rate constants ($k_{biof,ae,THCOH}$=21034 L gTSS^{-1} d^{-1},
586 $k_{biof,an,THCOH}$=5066 L gTSS^{-1} d^{-1}), which were also observed for THCCOOH bi-
587 otransformation in the anaerobic biofilm ($k_{biof,an,THCCOOH}$=3272 L gTSS^{-1} d^{-1}).

588 We note that the high k_{biof} values corresponded to high K_{df} values for these
589 chemicals (SI Table S4), a factor that makes THCOH and THCCOOH less bi-
590 oavailable for biotransformation. Interestingly, aerobic THCCOOH biotrans-
591 formation obtained ($k_{biof,ae,THCCOOH}$=133 L gTSS^{-1} d^{-1}) was lower than that un-
592 der anaerobic conditions.

593 **The impact of mass transfer limitation.** Compared to common growth sub-
594 strates, illicit drug biomarkers are relatively large molecules. The average mo-
595 lar volume, V_l (cm^{-3} mol^{-1}), of biomarkers in this study is 250 cm^{-3} mol^{-1}, sig-
596 nificantly larger than the molar volume of readily biodegradable substrates

17

597 such as acetate (56.1 cm^{-3}).[48] Therefore, the comparably high molar volume is
598 assumed to significantly impact diffusivity of drug biomarkers in biofilm.

599 In general, the concentration in the boundary layer is proportional to the ratio
600 of convective mass transfer (i.e. axial flow in biofilm reactor) to diffusive mass
601 transport (*Sh* number). According to eq. 5, molecules with a higher molar vol-
602 ume and low diffusivity are expected to have lower boundary layers (SI Figure
603 S1). In biofilm modeling studies, typically an average boundary layer is as-
604 sumed for all chemicals, under the condition that this approximation does not
605 impact the accuracy of predictions; this, however, is generally done without
606 proper error assessment. Figure 4 (Y-Z axis) illustrates the impact of the choice
607 of boundary layer thickness on the accuracy of estimation of biotransformation
608 rate, k_f, for the example of MEPH and HER in aerobic biofilms. Estimated
609 values for a range of boundary layer thicknesses (5 to 100 μm) together with
610 discretization number (10 to 100) were compared with reference predictions
611 for MEPH (30 μm) and HER (20 μm) with discretization number of 100. These
612 results indicate that the impact of the boundary layer thickness on parameter
613 estimates (i) is compound-specific; and (ii) varies by the discretization number
614 employed (Figure 4 X-Z axis). A higher influence was observed for more re-
615 active compounds, i.e. HER, at lower discretization numbers. In Figure 4, red
616 dots denote the values employed in this study (discretization number=80 lay-
617 ers; boundary layer thickness=23 μm). Furthermore, diffusion of HER and
618 MEPH was compared in aerobic and anaerobic biofilms through simulation of
619 diffusive transport, considering negligible partitioning to solids and transfor-
620 mation (SI Figure S12). Following the spiking of internal standards in BT-P1
621 experiments, the concentrations in the bulk phase of the reactors were predicted
622 to reach an equilibrium level after 2 h in aerobic biofilms and 4 h in anaerobic
623 biofilms. These delays show the impact of mass transfer limitation across the
624 boundaries of biofilm and liquid phase – a factor that necessitates an effective
625 diffusion modelling for which we provided an example here. Moreover, the
626 recirculation between external tank and reactor cause additional limiting step
627 for reaching equilibrium. An example of concentration profile inside the bio-
628 film is also presented for MEPH (SI, Figure S13).

629 **Transformation in raw wastewater and sewer biofilms – A comparison.**
630 Biotransformation rate constants in sewer biofilms k_{biof} estimated in this study
631 were compared rate constants in the presence of suspended solids, k_{bio} (Figure
632 5).[12] Under aerobic conditions (reproducing a gravity sewer), most biomarkers
633 exhibited similar k_{biof} and k_{bio} values (see error bars in Figure 5). Biofilm-me-
634 diated transformations were found to be dominant for COE and NCOE, whilst

635 the majority of MORG and MOR transformation occurred in the bulk water by
636 suspended biomass. Under anaerobic conditions, MEPH, METD, COC, EME,
637 CE, THCOH, and THCCOOH were found to be biotransformed only in bio-
638 films. Moreover, no additional major transformation products for HER and
639 MORG, other than 6MAM and MOR, respectively, were identified in the bio-
640 film reactors, as opposed to raw wastewater.

641 **Future perspectives.** In this study, we assessed the transformation of 16 drug
642 biomarkers in biofilm reactors under aerobic and anaerobic conditions, repre-
643 senting typical conditions in gravity and pressure sewers (respectively). This
644 investigation complemented our previous study[12] on the fate of drug bi-
645 omarkers in raw sewage, in the presence of suspended biomass only. A com-
646 parative assessment of the results indicates that sewer biofilms enhance the
647 transformation kinetics of many of selected drug biomarkers, particularly un-
648 der anaerobic conditions (Figure 5), likely due to higher anaerobic activity in
649 biofilms than in suspended biomass. Under aerobic conditions, transformation
650 kinetics in biofilms was overall comparable to that observed for untreated
651 sewage, indicating again limited stability of selected biomarkers. This evi-
652 dence suggests the necessity of accounting for biofilm-mediated transfor-
653 mation when predicting in-sewer fate of drug biomarkers. Moreover, for the
654 reliable prediction of trace organic chemical fate in biofilm, the mathematical
655 consistency of simulation model structures should be assessed.

656 More observations are needed to validate sorption and transformation of THC
657 in sewer biofilms. In this study all drug biomarkers (parents and metabolites)
658 were spiked simultaneously to simulate environmentally-relevant conditions,
659 i.e. the occurrence of drug biomarkers in sewer as a mixture. The developed
660 model however could describe the transformations among biomarkers. Never-
661 theless, future experimental designs used could benefit from spiking unrelated
662 biomarkers (e.g., in separate batch experiments) or using biomarkers with sev-
663 eral different labels, although resulting in a drastic increase of the cost of chem-
664 ical analysis.

665 The microbial activity of the two biofilms in this study was characterized by
666 monitoring utilization of primary substrates (e.g., organic carbon, sulfate) dur-
667 ing batch experiments. Our results showed substantial differences in microbial
668 activity between the two biofilms assessed in this study, e.g., significantly
669 higher sulfate-reducing activity in the anaerobic biofilm. In sewer systems, mi-
670 crobial functions and community of sewer biofilms vary over a sewer length
671 likely as a result of changes in boundary conditions and gradients in substrate

672 concentrations and wastewater composition. To date, this has been demon-
673 strated for gravity sewers[14]. Hence, further research is required to characterize
674 microbial activity of the sewer biofilms at different sewer locations and corre-
675 late the microbial community and activity with biotransformation rates.

676 In this study, the aeration was performed in a separate tank and not directly in
677 the biofilm reactor. The objective was to provide sufficient oxygen supply to
678 ensure that most microorganisms would be exposed to aerobic conditions. It
679 should be noted that (re)aeration may be different in full-scale sewer systems,
680 being caused by flow fluctuations and mixing. The current study potentially
681 offers the background for a combined modelling framework for real sewers,
682 where switching functions based on dissolved oxygen concentration would al-
683 low differentiating between aerobic and anaerobic conditions.

684 Although this study compared the biotransformation rate in raw wastewater
685 and in biofilms, the contribution of each of these biotransformation processes
686 to the overall drug biomarkers removal should be assessed. Moreover, the as-
687 sessment of drug abuse rates at catchment level should account for, im-
688 portantly, the layout of the sewer system, hydraulic conditions[49] and the possi-
689 ble drug release patterns. Additionally, model-based back-calculation tools
690 should account for abiotic processes and biotransformation induced by sus-
691 pended biomass and sewer biofilms.[50] Hence, a reactive-transport model needs
692 to be developed, describing drug biomarkers transformation under steady-state
693 and dynamic conditions. Transformation rates estimated in this study can be
694 used to calibrate such simulation models. Our ongoing research[50] is addressing
695 the impact of neglecting in-sewer biotransformation on estimation of daily
696 drug consumption in catchments using uncertainty analysis and measurements
697 from sampling campaigns. Results presented in this study underscore the high
698 level of complexity of in-sewer biomarker fate, of which the implications to
699 wastewater-based epidemiological engineering are numerous.

Acknowledgments

Reference

(1)   Thomas, K. V.; Bijlsma, L.; Castiglioni, S.; Covaci, A.; Emke, E.; Grabic, R.; Hernández, F.; Karolak, S.; Kasprzyk-Hordern, B.; Lindberg, R. H.; et al. Comparing illicit drug use in 19 European cities through sewage analysis. *Sci. Total Environ.* **2012**, *432*, 432–439.

(2)   Daughton CG. Illicit drugs in municipal sewage: proposed new non-intrusive tool to heighten public awareness of societal use of illicit/abused drugs and their potential for ecological consequences. In *American Chemical Society, Symposium Series*; American Chemical Society, Symposium Series: Washington, DC, 2001; p 348–364.

(3)   Hvitved-Jacobsen, T.; Vollertsen, J.; Matos, J. S. The sewer as a bioreactor - A dry weather approach. *Water Sci. Technol.* **2002**, *45* (3), 11–24.

(4)   Jelic, A.; Rodriguez-Mozaz, S.; Barceló, D.; Gutierrez, O. Impact of in-sewer transformation on 43 pharmaceuticals in a pressurized sewer under anaerobic conditions. *Water Res.* **2014**, *68*, 98–108.

(5)   McCall, A.-K.; Bade, R.; Kinyua, J.; Lai, F. Y.; Thai, P. K.; Covaci, A.; Bijlsma, L.; van Nuijs, A. L. N.; Ort, C. Critical review on the stability of illicit drugs in sewers and wastewater samples. *Water Res.* **2016**, *88*, 933–947.

(6)   Castiglioni, S.; Bijlsma, L.; Covaci, A.; Emke, E.; Hernández, F.; Reid, M.; Ort, C.; Thomas, K. V.; Van Nuijs, A. L. N.; De Voogt, P.; et al. Evaluation of uncertainties associated with the determination of community drug use through the measurement of sewage drug biomarkers. *Environ. Sci. Technol.* **2013**, *47* (3), 1452–1460.

(7)   van Nuijs, A. L. N.; Abdellati, K.; Bervoets, L.; Blust, R.; Jorens, P. G.; Neels, H.; Covaci, A. The stability of illicit drugs and metabolites in wastewater, an important issue for sewage epidemiology? *J. Hazard. Mater.* **2012**, *239–240*, 19–23.

(8)   Senta, I.; Krizman, I.; Ahel, M.; Terzic, S. Assessment of stability of drug biomarkers in municipal wastewater as a factor influencing the estimation of drug consumption using sewage epidemiology. *Sci. Total Environ.* **2014**, *487*, 659–665.

(9)   Baker, D. R.; Očenášková, V.; Kvicalova, M.; Kasprzyk-Hordern, B. Drugs of abuse in wastewater and suspended particulate matter - Further developments in sewage epidemiology. *Environ. Int.* **2012**, *48*, 28–38.

(10)   Baker, D. R.; Kasprzyk-Hordern, B. Critical evaluation of methodology commonly used in sample collection, storage and preparation for the analysis of pharmaceuticals and illicit drugs in surface water and wastewater by solid phase extraction and liquid chromatography-mass spectrometry. *J. Chromatogr. A* **2011**, *1218* (44), 8036–8059.

(11)   Polesel, F.; Andersen, H. R.; Trapp, S.; Plósz, B. G. Removal of Antibiotics in Biological Wastewater Treatment Systems □ A Critical Assessment Using the Activated Sludge Modeling Framework for Xenobiotics (ASM-X). *Environ. Sci. Technol.* **2016**, *50* (19), 10316−10334.

(12)   Ramin, P.; Brock, A. L.; Polesel, F.; Causanilles, A.; Emke, E.; de Voogt, P.; Plósz, B. G. Transformation and sorption of illicit drug biomarkers in sewer systems: understanding the role of suspended solids in raw wastewater. *Environ. Sci. Technol.* **2016**, *50* (24), 13397–13408.

(13)   Thai, P. K.; Jiang, G.; Gernjak, W.; Yuan, Z.; Lai, F. Y.; Mueller, J. F. Effects of

21

750 sewer conditions on the degradation of selected illicit drug residues in wastewater.
751 *Water Res.* **2014**, *48*, 538–547.

752 (14) McCall, A.-K.; Scheidegger, A.; Madry, M. M.; Steuer, A. E.; Weissbrodt, D. G.;
753   Vanrolleghem, P. A.; Kraemer, T.; Morgenroth, E.; Ort, C. Influence of different
754   sewer biofilms on transformation rates of drugs. *Environ. Sci. Technol.* **2016**, *50* (24),
755   13351–13360.

756 (15) Ort, C.; Gujer, W. Sorption and high dynamics of micropollutants in sewers. *Water
757   Sci. Technol.* **2008**, *57* (11), 1791–1797.

758 (16) Plósz, B. G.; Reid, M. J.; Borup, M.; Langford, K. H.; Thomas, K. V.
759   Biotransformation kinetics and sorption of cocaine and its metabolites and the factors
760   influencing their estimation in wastewater. *Water Res.* **2013**, *47* (7), 2129–2140.

761 (17) Bisceglia, K. J.; Lippa, K. a. Stability of cocaine and its metabolites in municipal
762   wastewater - the case for using metabolite consolidation to monitor cocaine
763   utilization. *Environ. Sci. Pollut. Res.* **2014**, *21* (516), 4453–4460.

764 (18) Jiang, F.; Leung, D. H.-W. W.; Li, S.; Chen, G.-H. H.; Okabe, S.; van Loosdrecht, M.
765   C. M. A biofilm model for prediction of pollutant transformation in sewers. *Water
766   Res.* **2009**, *43* (13), 3187–3198.

767 (19) Schwarzenbach, R. P.; Gschwend, P. M.; Imboden, D. M. *Environmental Organic
768   Chemistry*; Wiley Interscience: Hoboken, NJ, 2003.

769 (20) Wicke, D.; Böckelmann, U.; Reemtsma, T. Experimental and modeling approach to
770   study sorption of dissolved hydrophobic organic contaminants to microbial biofilms.
771   *Water Res.* **2007**, *41* (10), 2202–2210.

772 (21) Torresi, E.; Polesel, F.; Bester, K.; Christensson, M.; Smets, B. F.; Trapp, S.;
773   Andersen, H. R.; Plósz, B. G. Diffusion and sorption of organic micropollutants in
774   biofilms with varying thicknesses. *Water Res.* **2017**.

775 (22) Huisman, J. L.; Gujer, W. Modelling wastewater transformation in sewers based on
776   ASM3. *Water Sci. Technol.* **2002**, *45* (6), 51–60.

777 (23) EMCDDA. *European Drug Report*; 2017.

778 (24) Boerner, U.; Abbott, S.; Roe, R. L. The Metabolism of Morphine and Heroin in Man.
779   *Drug Metab. Rev.* **1975**, *4* (1), 39–73.

780 (25) Rochex, A.; Godon, J.; Bernet, N.; Escudie, R. Role of shear stress on composition ,
781   diversity and dynamics of biofilm bacterial communities. *Water Res.* **2008**, *42*, 4915–
782   4922.

783 (26) Oms, C.; Gromaire, M. C.; Saad, M.; Milisic, V.; Chebbo, G.; Gromaire, M. C.; Saad,
784   M.; Milisic, V.; Bed, G. C. Bed shear stress evaluation in combined sewers. *Urban
785   Water J.* **2008**, *5* (3), 219–229.

786 (27) *APHA. Standard methods for the examination of water and wastewater. American
787   Public Health Association*, 19th ed.; Washington, D.C, 1995.

788 (28) Bijlsma, L.; Emke, E.; Hernández, F.; de Voogt, P. Performance of the linear ion trap
789   Orbitrap mass analyzer for qualitative and quantitative analysis of drugs of abuse and
790   relevant metabolites in sewage water. *Anal. Chim. Acta* **2013**, *768* (1), 102–110.

791 (29) Horn, H.; Hempel, D. C. Modeling mass transfer and substrate utilization in the

792   boundary layer of biofilm systems. *Water Sci. Technol.* **1998**, *37* (4–5), 139–147.

793   (30) Othmer, D. F.; Thakar, M. S. Correlating Diffusion Coefficients in Liquids. *Ind. Eng.*
794   *Chem.* **1953**, *45* (3), 589–593.

795   (31) Hayduk, W.; Laudie, H. Prediction of diffusion coefficients for nonelectrolytes in
796   dilute aqueous solutions. *AIChE J.* **1974**, *20* (3), 611–615.

797   (32) Guimerà, X.; Dorado, A. D.; Bonsfills, A.; Gabriel, G.; Gabriel, D.; Gamisans, X.
798   Dynamic characterization of external and internal mass transport in heterotrophic
799   biofilms from microsensors measurements. *Water Res.* **2016**, *102*, 551–560.

800   (33) Wanner, O.; Eberl, H. J.; Morgenroth, E.; Noguera, D. R.; Picioreanu, C.; Rittmann,
801   B. E.; van Loosdrecht, M. C. . *Mathematical modeling of biofilms*; 2006.

802   (34) Recktenwald, A.; Lücke, M.; Müller, H. W. Taylor vortex formation in axial through-
803   flow: Linear and weakly nonlinear analysis. *Phys. Rev. E* **1993**, *48* (6), 4444–4454.

804   (35) Castiglioni, S.; Zuccato, E.; Fanelli, R. *Illicit Drugs in the Environment: Occurrence,*
805   *Analysis, and Fate Using Mass Spectrometry*; JohnWiley & Sons, Inc, 2011.

806   (36) Laloy, E.; Vrugt, J. a. High-dimensional posterior exploration of hydrologic models
807   using multiple-try DREAM(ZS) and high-performance computing. *Water Resour.*
808   *Res.* **2012**, *48* (1), 1–18.

809   (37) Ramin, P.; Valverde-Pérez, B.; Polesel, F.; Locatelli, L.; Plósz, B. G. A systematic
810   model identification method for chemical transformation pathways – the case of
811   heroin biomarkers in wastewater. *Sci. Report, Accept. with Revis.* **2017**.

812   (38) Vangsgaard, A. K.; Mauricio-Iglesias, M.; Gernaey, K. V.; Smets, B. F.; Sin, G.
813   Sensitivity analysis of autotrophic N removal by a granule based bioreactor: Influence
814   of mass transfer versus microbial kinetics. *Bioresour. Technol.* **2012**, *123*, 230–241.

815   (39) Sin, G.; Gernaey, K. V.; Neumann, M. B.; van Loosdrecht, M. C. M.; Gujer, W.
816   Uncertainty analysis in WWTP model applications: A critical discussion using an
817   example from design. *Water Res.* **2009**, *43* (11), 2894–2906.

818   (40) Rosa Boleda, M.; Huerta-Fontela, M.; Ventura, F.; Galceran, M. T. Evaluation of the
819   presence of drugs of abuse in tap waters. *Chemosphere* **2011**, *84* (11), 1601–1607.

820   (41) Plósz, B. G.; Langford, K. H.; Thomas, K. V. An activated sludge modeling
821   framework for xenobiotic trace chemicals (ASM-X): Assessment of diclofenac and
822   carbamazepine. *Biotechnol. Bioeng.* **2012**, *109* (11), 2757–2769.

823   (42) Torresi, E.; Fowler, J. S.; Polesel, F.; Bester, K.; Andersen, H. R.; Smets, B. F.; Plósz,
824   B. G.; Christensson, M. Biofilm thickness influences biodiversity in nitrifying
825   MBBRs – Implications on micropollutant removal. *Environ. Sci. Technol.* **2016**, *50*
826   (17), 9279–9288.

827   (43) Sathyamoorthy, S.; Chandran, K.; Ramsburg, C. A. Biodegradation and Cometabolic
828   Modeling of Selected Beta Blockers during Ammonia Oxidation. *Environ. Sci.*
829   *Technol.* **2013**, *47*, 12835−12843.

830   (44) Bisceglia, K. J.; Roberts, A. L.; Lippa, K. A. A hydrolysis procedure for the analysis
831   of total cocaine residues in wastewater. *Anal. Bioanal. Chem.* **2012**, *402*, 1277–1287.

832   (45) Bisceglia, K. J. K.; Lippa, K. a. Stability of cocaine and its metabolites in municipal
833   wastewater - the case for using metabolite consolidation to monitor cocaine

23

834   utilization. *Environ. Sci. Pollut. Res.* **2014**, *21* (6), 4453–4460.

835   (46) Stefanidou, M.; Athanaselis, S.; Spiliopoulou, C.; Dona, A.; Maravelias, C.
836   Biomarkers of opiate use. *Int. J. Clin. Pract.* **2010**, *64* (12), 1712–1718.

837   (47) Castiglioni, S.; Zuccato, E.; Crisci, E.; Chiabrando, C.; Fanelli, R.; Bagnati, R.
838   Identification and measurement of illicit drugs and their metabolites in urban
839   wastewater by liquid chromatography-tandem mass spectrometry. *Anal. Chem.* **2006**,
840   *78* (24), 8421–8429.

841   (48) ACD/I-Lab 2.0 Prediction Software by Advanced Chemistry Development Inc.
842   (ACD/Labs).

843   (49) Mccall, A.; Palmitessa, R.; Blumensaat, F.; Morgenroth, E.; Ort, C. Modeling in-
844   sewer transformations at catchment scale – Implications on drug consumption
845   estimates in wastewater-based epidemiology. *Water Res.* **2017**.

846   (50) Ramin, P. Modelling Illicit Drug Fate in Sewers for Wastewater-Based
847   Epidemiology, PhD Thesis, Technical University of Denmark, 2016.

848

849

850 **Table 1.** Model state variables and parameters

| Symbol	Definition	Units	Values
A_b	Biofilm area	m^2	4.10^{-3}
C_R	Concentration of drug biomarkers in reactor	g L^{-1}	
C_b	Concentration of drug biomarkers inside biofilm	g L^{-1}	
C_T	Concentration of drug biomarkers in external tank bulk phase	g L^{-1}	
C_{Tw}	Concentration of drug biomarkers sorbed onto external tank wall	g L^{-1}	
d	Gap between rotating drum and stationary cylinder (R_2-R_1)	m	0.012
d_R	Reactor Characteristic length (2d)		0.024
D	Diffusion coefficient of the soluble compounds into the biofilm	m^2 d^{-1}	Table S2
D_w	Diffusion coefficient of the soluble compounds in water	m^2 d^{-1}	Table S2
f	Dimensionless effective diffusivity	-	ae:0.68 an:0.38
j_b	Flux of compounds between bulk phase and the biofilm	g m^{-2} d^{-1}	
k_b	Mass transfer coefficient between bulk phase and the biofilm	m d^{-1}	
$k_{des,w}$	Desorption from reactor wall	d^{-1}	100
K_{dw}	Reactor wall–liquid partition coefficient	m^3 m^{-2}	Ramin et al.[12]
K_d	Suspended Solid–liquid partition coefficient	L gTSS^{-1}	Ramin et al.[12]
K_{df}	Suspended biofilm–liquid partition coefficient	L gTSS^{-1}	Table S4
k_{abio}	Abiotic transformation rate constant	d^{-1}	Ramin et al.[12]
k_{bio}	TSS-normalized biotransformation rate constant	L gTSS^{-1} d^{-1}	Ramin et al.[12]
k_f	Sewer biofilm biotransformation rate (eq. 9)	d^{-1}	Figure S11
k_{biof}	TSS-normalized Sewer biofilm biotransformation rate	L gTSS^{-1} d^{-1}	Table S4
k'_{biof}	Area-to-volume-normalized Sewer biofilm biotransformation rate	m^3 m^{-2} d^{-1}	Table S4
L_b	Concentration boundary layer	m	23.10^{-6}
M	Biomarker molecular weight	g mol^{-1}	Table S2
O	Observed (measured) values		
P	Predicted (simulated) values		
$Q_{in,R}$	Reactor inflow	m^3 d^{-1}	4.10^{-3}
$Q_{out,R}$	Reactor outflow	m^3 d^{-1}	4.10^{-3}
$Q_{in,T}$	External tank inflow	m^3 d^{-1}	4.10^{-3}
$Q_{out,T}$	External tank outflow	m^3 d^{-1}	4.10^{-3}
r_R	Reaction rate in reactor	g L d^{-1}	
r_b	Reaction rate in side biofilm	g L d^{-1}	
r_T	Reaction rate in external tank	g L d^{-1}	
R_1	Reactor inner radios (outer radios of rotating drum)	m	0.045
R_2	Reactor outer radios (inner radios of stationary cylinder)	m	0.057
V_R	Total reactor volume	m^3	9.61.10^{-4}
$\bar{u}$	Average axial velocity inside reactor (a continuous operation; b: batch experiment)	m s^{-1}	a: 0.12.10^{-4} a: 2.89.10^{-4}
V_b	Biofilm volume	m^3	ae: 1. 25.10^{-4} an: 1.71.10^{-4}
V_T	Bulk volume in external volume	m^3	Figure S2
V_l	Molar volume	cm^3 g mole^{-1}	Table S2
X_{SS}	Concentration of suspended solids	gTSS L	Table S3
ΔZ	Discretization distance inside biofilm for spatial discretization of partial differential equations	m	ae:9.3 10^{-6} an: 12.8 10^{-6}
μ_w	Dynamic viscosity of water (at ~17° C)	kg m^{-1} s^{-1}	1.07 10^{-3}
ν	Kinematic viscosity of water (at ~17° C)	m^{-2} s^{-1}	1.07 10^{-6}
σ_w	Wet-surface-to-volume ratio	m^2 m^{-3}	Figure S2
Ω	Angular velocity of rotating drum	rad d^{-1}	2.09

851

852

853
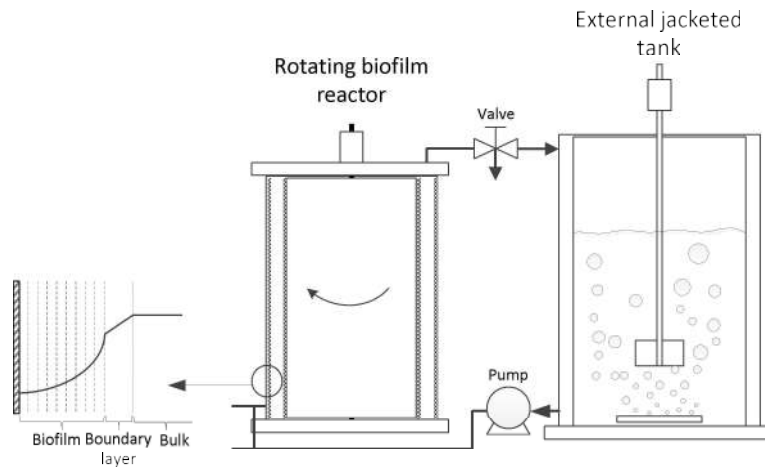
854 **Figure 1**. Configuration of rotating biofilm reactor (on the left) connected to an external tank (on
855 the right) during batch experiments. The samples were taken from the outlet of the biofilm reac-
856 tor, on the top valve. Anaerobic or aerobic conditions were maintained in the external tank by
857 sparging air or nitrogen, respectively, from a diffuser placed at the bottom of the tank. A typical
858 drug concentration profile inside the biofilm is also presented.

859
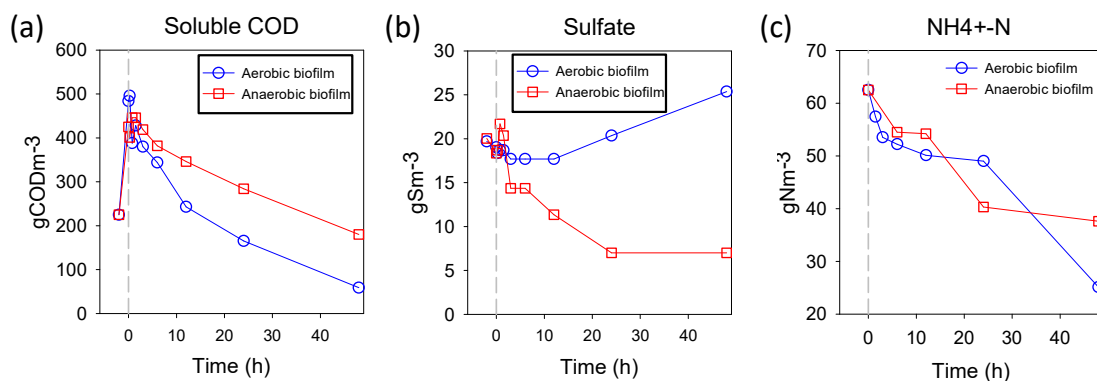
860

861 **Figure 2**. Soluble COD, sulfate and ammonium concentrations measured during BT-P1 ex-
862 periments under aerobic and anaerobic conditions. Measurements before t=0 refer to samples
863 taken prior to the spiking of standards, and the subsequent increase of soluble COD concen-
864 tration at t=0 should be associated with the addition of MeOH resulting from spiking of
865 biomarkers mixture. Lines connecting data points are based on simple linear interpolation to
866 show the trends.

867
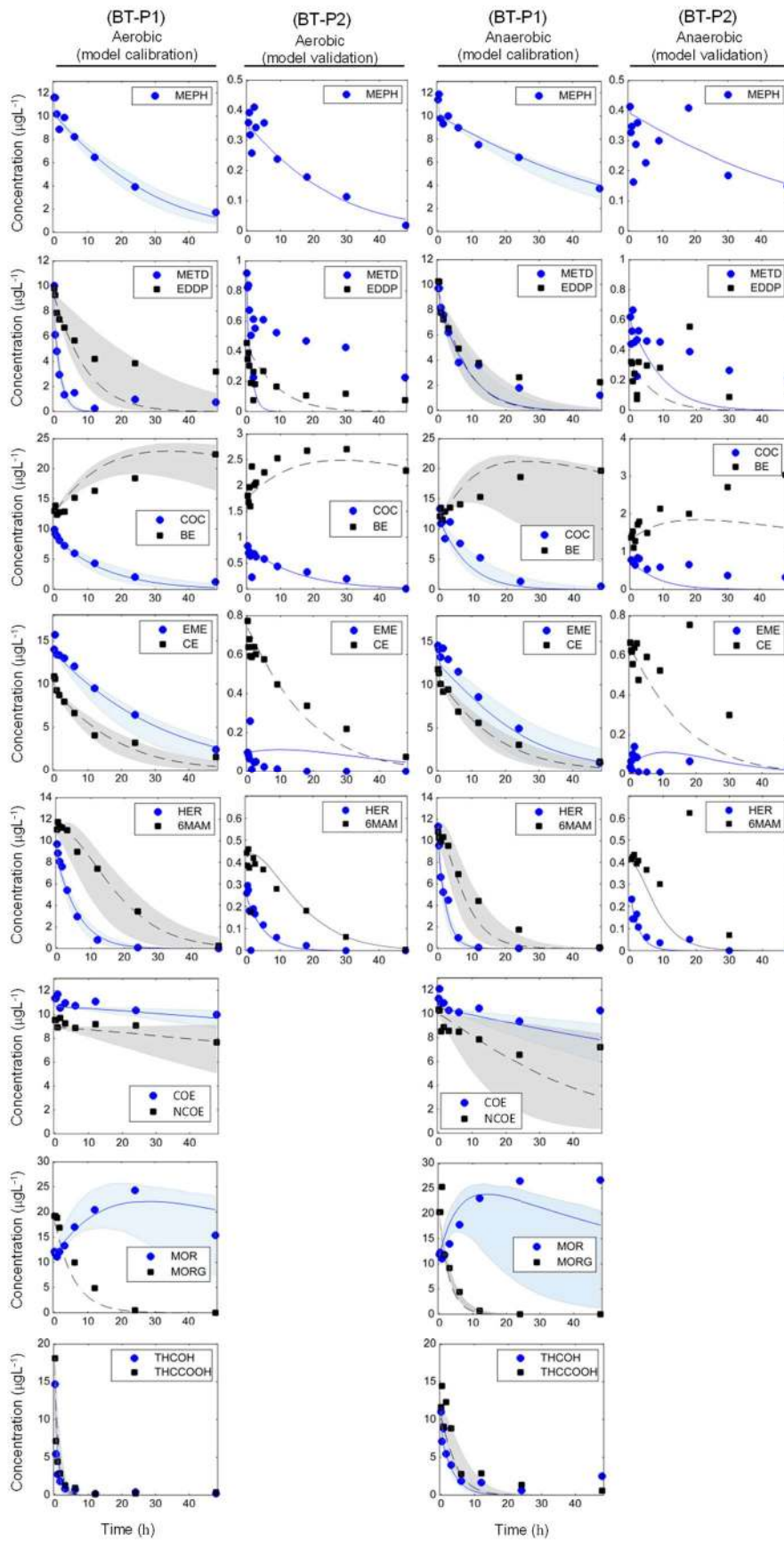
869 **Figure 3.** Experimental data and simulation results for biomarker transformations in sewer
870 biofilm under aerobic and anaerobic conditions. Results are related to model calibration us-
871 ing BT-P1 experimental data and model validation using BT-P2 experimental data. THC
872 data is presented in (SI, Figure S10). Markers are measured data and lines are simulation
873 results. The shaded areas reflect 95% credibility interval of model prediction.

884
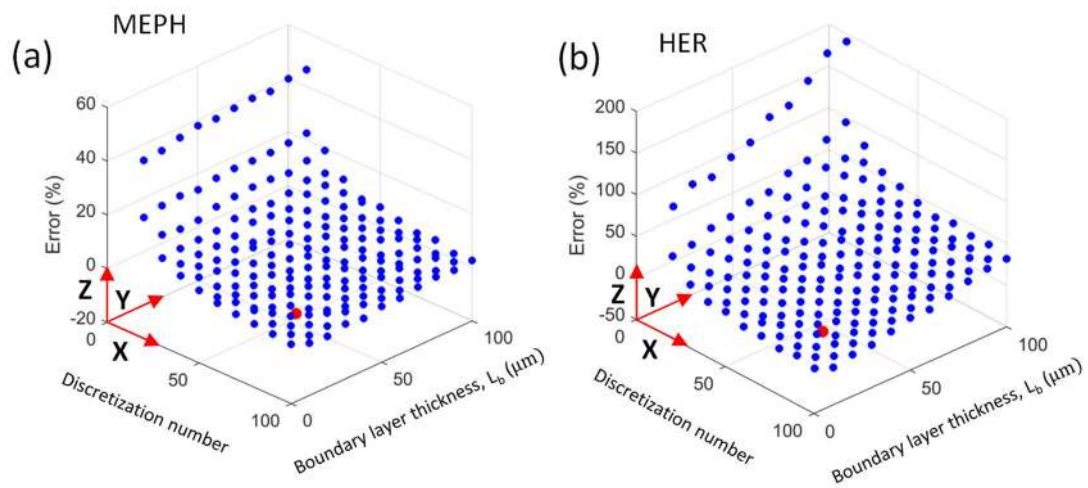
Figure 4. The impact of discretization number (number of discretization layers considered for numerical integration in biofilm) and boundary layer thickness on estimation of aerobic transformation rate, k_f (d^{-1}), for MEPH and HER. 190 scenarios were considered for each chemical. The parameter estimate at each scenario was compared with the reference scenario for each chemical. The reference scenario contained 100 layers using the accurate estimation of boundary layer thickness, i.e. 30 μm for MEPH and 20 μm for HER. Blue dots are the data resulted from scenarios and red dots correspond to the values chosen in this study (i.e. 80 discretization number and 23 μm boundary layer thickness). Considering this choice resulted in an acceptable error i.e. 0.4% for MEPH and 2% for HER.
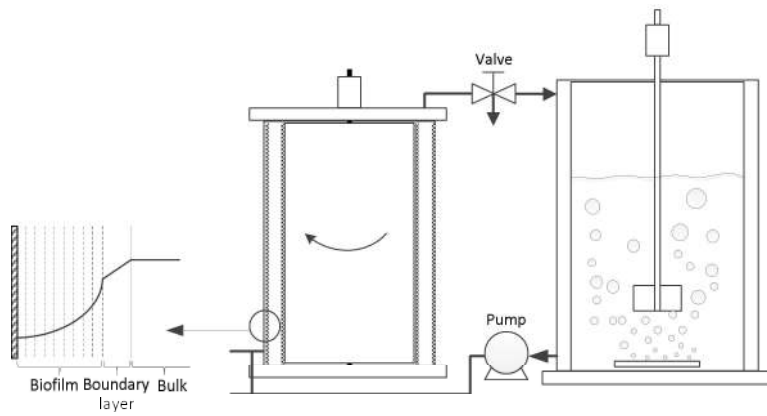
884
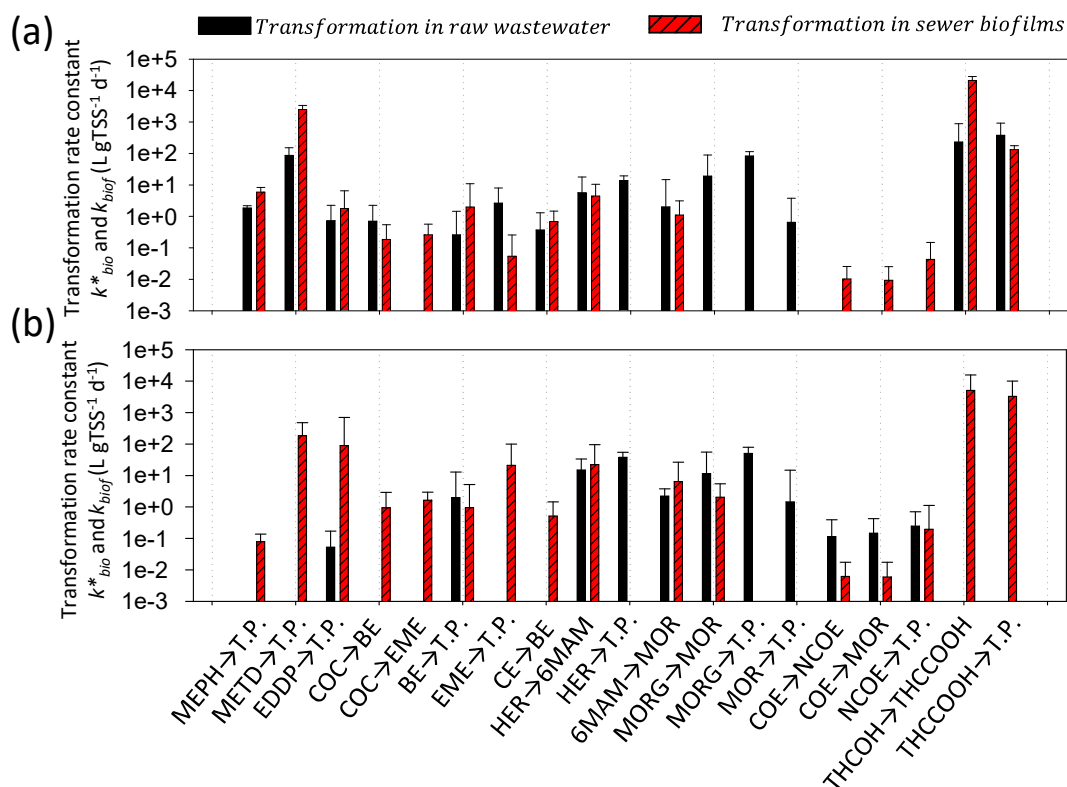
Figure 5. Comparing the biotransformation of drug biomarkers in raw wastewater and bio-transformation in sewer biofilms under aerobic (a), and anaerobic (b) conditions. For this comparison, TSS-normalized transformation rate constants in raw wastewater k_{bio} (L gTSS^{-1} d^{-1}) reported in Ramin et al.[12] are compared with sewer biofilm-mediated transformation rate constants, k_{biof} (L gTSS^{-1} d^{-1}), from this study. Error bars identify the upper bound of the 95% credibility interval of estimated parameters.

892 **TOC/graphical abstract**

893